CONDENSED MATTER

Metastable Semimetallic Solid Atomic Phase of Nitrogen

K. S. Grishakov[a, b,] * and N. N. Degtyarenko[a]

[a] National Research Nuclear University MEPhI (Moscow Engineering Physics Institute), Moscow, 115409 Russia
[b] Research Institute for the Development of Scientific and Educational Potential of Youth, Moscow, 119620 Russia
*e-mail: ksgrishakov@mephi.ru

A new solid atomic phase of nitrogen, which is dynamically stable at pressures above 20 GPa, has been predicted within the density functional theory. This phase has a low symmetry of the crystal lattice $P\bar{1}$ and exhibits electronic properties unique for nitrogen crystal structures in the low-pressure region, which are characteristic of semimetals. The structural, energy, mechanical, and electronic properties of this phase are calculated and compared with similar characteristics of the gauche phase of nitrogen.

INTRODUCTION

In nature, nitrogen exists in the form of diatomic molecules N_2 with a strong triple covalent bond. One of the important features of nitrogen is the ratio between triple and single bond energies, which is not typical of many other elements; the sum of three single bond energies is approximately 1.5 times less than the triple bond energy [1]. Thus, energy can be stored by creating a nitrogen-containing substance in which the nitrogen atoms are linked to each other by single bonds. In this regard, pure nitrogen clusters and crystal structures with single bonds between atoms are of the greatest interest, and according to theoretical predictions, their efficiency is several times higher than those of other high-energy substances [1, 2]. The molecular phase of nitrogen under normal conditions is more thermodynamically stable compared to nitrogen clusters and crystalline structures; therefore, nonmolecular structures tend to decompose into diatomic molecules with the release of a large amount of energy. This process occurs without the formation of polluting compounds, since molecular nitrogen is the main component of atmospheric air. Therefore, various nonmolecular nitrogen structures are considered as environmentally friendly materials with a high stored energy density.

Over the past decades, numerous theoretical and experimental studies have been carried out to search for nonmolecular nitrogen structures, as well as to study their properties and stability. To date, the stability of many different isolated N_m clusters, $m = 3-78$, is theoretically predicted [3–13]. However, the experimental production of such structures remains a rather difficult task, and only a few nitrogen clusters have already been synthesized: N_8 [14], N_4 [3, 15], N_3^- [16], N_5^+ [5], and N_5^- [4].

At high pressures, the molecular phase of nitrogen is transformed into a solid atomic state, which is also actively studied along with cluster forms of nitrogen. The possibility of existence of a crystalline state of nitrogen with single bonds between atoms was first theoretically predicted in [17]. The predicted nitrogen structure has the crystal lattice symmetry $I2_13$ [17] and is called the cubic gauche phase of nitrogen (*cg*-N). Further theoretical calculations predicted many different solid phases of nitrogen [18–26]. Among all theoretically predicted nitrogen crystal structures at pressures below 150 GPa, the gauche phase of nitrogen is the most thermodynamically favorable [25, 27, 28]. Modeling of decompression at zero temperature demonstrated that only the *cg*-N [17], *Pccn* [35], $R\bar{3}$ [24], and $P\bar{6}2c$ [25] phases are dynamically stable at low pressures. All theoretically considered solid phases of nitrogen, at least up to 400 GPa, have the electronic properties characteristic of semiconductors or insulators; therefore, they must be transparent to optical radiation of the corresponding wavelength. The $R\bar{3}$ phase has the smallest band gap [24].

The solid phase of nitrogen in the amorphous state was first synthesized in 2001 by compressing molecular nitrogen in a diamond anvil cell [29]. By gradually reducing the pressure and maintaining the temperature below 100 K, nitrogen in this amorphous state was kept for a certain time up to atmospheric pressure. This state exhibited semiconductor properties and, at pressures of ~240 GPa, demonstrated a band gap of ~0.4 eV. Subsequently, at a pressure above 110 GPa and a temperature above 2000 K, a polymeric phase of

nitrogen with first-order bonds and the structure corresponding to the theoretically predicted gauche phase of nitrogen was experimentally obtained [30, 31]. Other solid atomic phases of nitrogen such as the layered polymer phase LP-N [32], the phase with black phosphorus structure [33], the nitrogen structure similar to the previously theoretically predicted *Pba*2 phase [28], and the hexagonal layered polymer phase HLP-N [34] were also synthesized at high pressures. In all experiments, attempts to decompress the samples to normal pressure led to the destruction of the nonmolecular phase.

Thus, despite active research, the experimental synthesis of solid atomic nitrogen structures stable under almost normal conditions is an unsolved problem. Therefore, one of the topical research directions is the search for new solid phases of nitrogen with single bonds between atoms, which are stable at low pressures (<50 GPa). Since various global optimization algorithms have already been actively used to predict nitrogen structures (e.g., evolutionary algorithm), which allowed the detection of a number of crystalline phases of nitrogen (see, e.g., [21, 25, 28]), further theoretical search for new structures stable at low pressures using such algorithms is significantly difficult, and new approaches are required.

In this work, the adiabatic compression of various crystals formed by nitrogen clusters at zero temperature was simulated to search for new solid phases of nitrogen. This approach is more "physical" than using global optimization algorithms and allows one to establish the effect of the precursor on the possibility of forming a stable solid phase under pressure. The use of this technique made it possible to discover a new crystalline phase of atomic nitrogen which is stable at low pressures (<50 GPa). Its structural, electronic, and mechanical properties are studied in detail and compared with similar characteristics of the gauche phase of nitrogen, which is the most thermodynamically favorable among other solid atomic structures of nitrogen at low pressures and is also experimentally synthesized.

CALCULATION METHOD

The calculations were carried out within the density functional theory using the Quantum ESPRESSO (QE) 6.7 package [35, 36]. The exchange-correlation functional PBEsol was used and the optimized norm-conserving Vanderbilt pseudopotential was obtained using the ONCVPSP 3.3.1 code [37]. The cutoff energy was 90 Ry, and the distance between k-points did not exceed 0.025 Å^{-1}. Test calculations performed with other cutoff energies and grids in k-space showed that the use of the values chosen for these parameters in calculations is sufficient to obtain results with a relative error of less than 1%. The thermo_pw code was used to calculate the elastic constants [38]. The path

between the points of high symmetry in the Brillouin zone for the plots of the electronic band structure and the phonon spectrum was obtained using the SeeK-path [39]. The symmetry of the crystal lattice was determined with an accuracy of 10^{-4} Å.

The technique for modeling the process of adiabatic compression of nitrogen structures at zero temperature was as follows: at a given pressure, geometric optimization of the crystal structure was carried out, and then the resulting relaxed configuration was used as the initial configuration for starting at a higher pressure. The pressure step was 20 GPa.

The Gibbs energy was calculated by the formula $G = E_{tot} + PV + F_{ph}(T)$, where $F_{ph}(T)$ is the phonon free energy found in the quasi-harmonic approximation, P is the pressure, V is the volume, and E_{tot} is the total energy.

RESULTS

We simulated the process of adiabatic compression at zero temperature for various crystal structures, the unit cell of which contained two nitrogen clusters. An example of such a crystal structure, consisting of $N_6(C_{2v})$-A clusters, is demonstrated in Fig. 1a. As a result of such simulation, the structure consisting of $N_6(C_{2v})$-A clusters, at a pressure of 160 GPa, was transformed into the three-dimensional solid atomic phase with the crystal lattice symmetry $P\bar{1}$ (see Figs. 1b and 1c). Since we were interested in the possibility of maintaining the solid atomic state at low pressures, the decompression of the $P\bar{1}$ phase was simulated down to zero pressure. Other cluster structures were transformed under pressure into quasi-one-dimensional structures, consisting of chains of connected clusters, and became dynamically unstable. For this reason, they will not be considered in this work.

Calculations of phonon spectra for the solid atomic phase of nitrogen with $P\bar{1}$ symmetry demonstrated that this structure is unstable at pressures below 20 GPa, as evidenced by the presence of imaginary frequencies in the phonon spectrum. At pressures from 20 to 200 GPa, the $P\bar{1}$ phase is dynamically stable, which, for a pressure of 20 GPa, is demonstrated in Fig. 2, where the phonon spectrum and the phonon density of states with $\omega^2(k) > 0$ are shown.

The structural parameters of the unit cell for the $P\bar{1}$ phase at a pressure of 20 GPa are presented in Table 1. Figure 3 demonstrates the pressure dependence of the bond length in the $P\bar{1}$ structure (when calculating these dependences, only three nearest neighbors are taken into account, which corresponds to the case of a single bond between atoms). The low symmetry of this phase leads to a large spread in bond lengths and bond angles. As the pressure increases, the
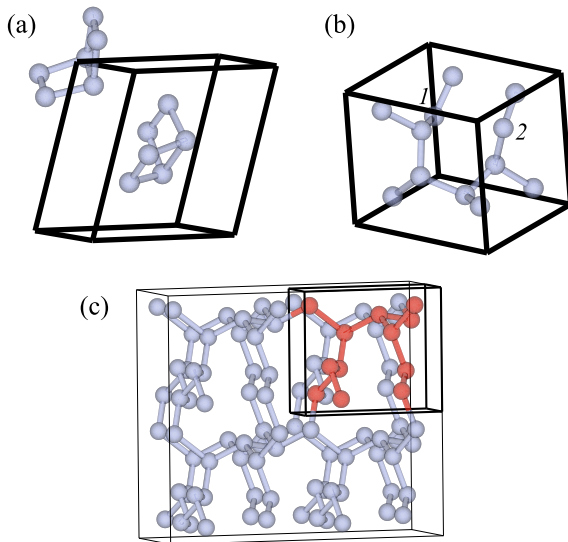
Fig. 1. (Color online) (a) Unit cell of the structure consisting of two $N_6(C_{2v})$-A nitrogen clusters, (b) unit cell of the solid atomic phase of nitrogen with the crystal lattice symmetry $P\bar{1}$, and (c) supercell $2 \times 2 \times 2$ of the solid phase $P\bar{1}$ (unit cell atoms are marked in red).

Fig. 2. Phonon spectrum and phonon density of states for the solid atomic phase $P\bar{1}$ of nitrogen.

$P\bar{1}$ phase becomes much more uniform in terms of the bond length between the atoms. The dependences shown in Fig. 3 indicate that the structure contains atoms with one of the three bond lengths ranging from 1.75 Å at a pressure of 200 GPa to 2.1 Å at a pressure of 20 GPa (these atoms are marked *1* and *2* in Fig. 1b); i.e., such a bond is in fact very weak or completely absent. For comparison, the gauche phase of cg-N nitrogen has the same bond length for all atoms: L_{bond} = 1.382, 1.362, 1.338, and 1.306 Å for pressures of 20, 50, 100, and 200 GPa, respectively.

The mechanical properties of the $P\bar{1}$ and cg-N phases at various pressures are summarized in Table 2. With the exception of the Poisson ratio, the elastic moduli for the $P\bar{1}$ phase are smaller than those for the gauche phase of the cg-N nitrogen. Thus, the "rigid-
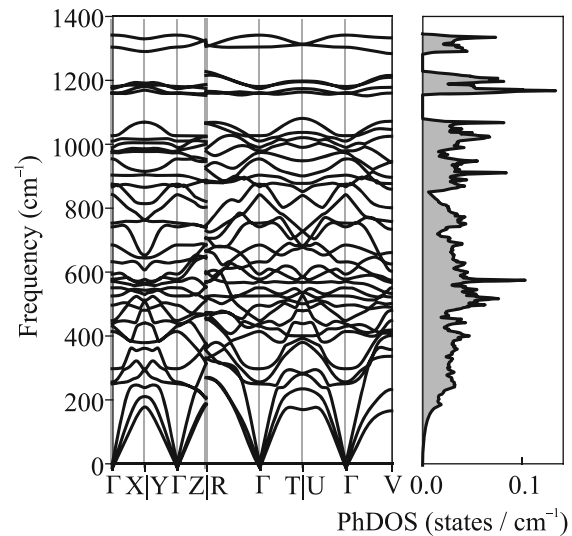
ity" of bonds between atoms in the $P\bar{1}$ phase should be less than that for the cg-N structure, and, consequently, pressure-induced deformation in the former phase should be larger. For example, when the pressure changes from 20 to 200 GPa, the volume per atom in the $P\bar{1}$ and cg-N phases decreases by 2.0 and 1.6 Å^3/atom, respectively.

The Gibbs energy per atom G in the $P\bar{1}$ crystalline phase was determined in the pressure range of 20–200 GPa. Figure 4 demonstrates the pressure dependences for various atomic solid phases of nitrogen that are dynamically stable at low pressures. For each pressure value in Fig. 4, the corresponding Gibbs energy of the cg-N gauche phase of nitrogen is chosen as the reference point. Among the solid atomic phases of nitrogen, the cg-N structure has the lowest Gibbs energy G in the entire considered pressure range. The Gibbs energy in the $P\bar{1}$ phase is slightly below the value for the $R\bar{3}$ structure. Since the Gibbs energy for the semi-metallic phase with the crystal lattice symmetry $P\bar{1}$ is

Table 1. Structural parameters of the unit cell of the $P\bar{1}$ phase, consisting of 12 nitrogen atoms, at a pressure of 20 GPa

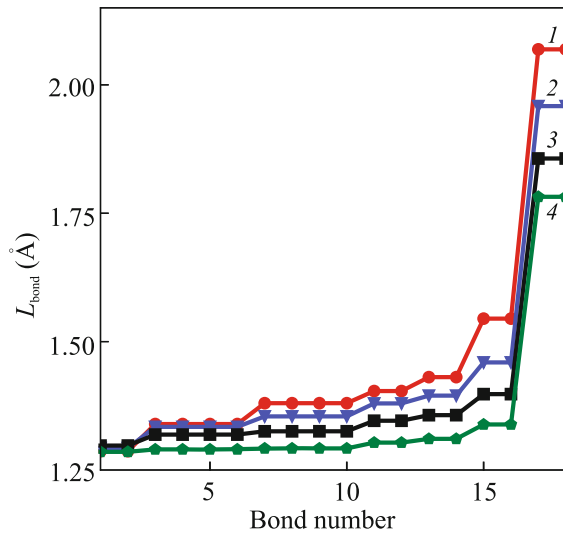| Lattice parameters	Atomic coordinates (arbitrary units)
$a = b = 4.1527$ Å, $c = 4.6485$ Å, $\alpha = \beta = 89.0°$, $\gamma = 89.9°$	(0.1719, 0.8796, 0.7194); (0.1204, 0.8281, 0.2806); (0.1488, 0.1403, 0.1765); (0.8645, 0.2776, 0.1192); (0.7224, 0.1355, 0.8808); (0.8597, 0.8512, 0.8235); (0.3512, 0.3597, 0.3235); (0.6355, 0.2224, 0.3808); (0.7776, 0.3645, 0.6192); (0.6403, 0.6488, 0.6765); (0.3281, 0.6204, 0.7806); (0.3796, 0.6719, 0.2194)

Fig. 3. (Color online) Bond lengths L_{bond} in a solid atomic structure $P\bar{1}$ at pressures of (*1*) 20, (*2*) 50, (*3*) 100, and (*4*) 200 GPa.
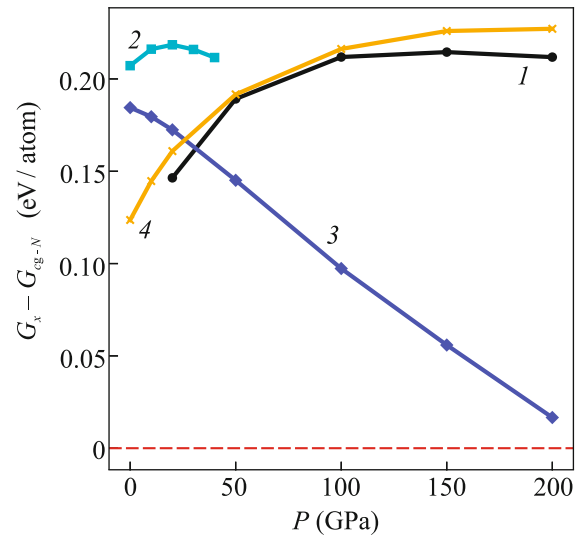

Fig. 4. (Color online) Pressure dependence of the difference in the Gibbs energy $G_X - G_{cg\text{-N}}$ per atom at $T = 300$ K between the solid atomic phases of nitrogen $X = $ (*1*) $P\bar{1}$, (*2*) $P\bar{6}2c$, (*3*) $Pccn$, and (*4*) $R\bar{3}$, and the gauche phase cg-N. The presented curves are shown for the region of dynamic stability of the corresponding nitrogen structures.

higher than that for the gauche phase of nitrogen, the $P\bar{1}$ phase is potentially capable of storing more energy.

It is known that the PBE functional can underestimate the band gap; for this reason, the HSE06 hybrid functional was used to calculate the electronic spectra for the $P\bar{1}$ structure. At a pressure of 20 GPa, the nitrogen phase $P\bar{1}$ exhibits semiconductor properties, and the band gap is 0.22 eV (see Fig. 5a). However, as the pressure increases to 50 GPa, the $P\bar{1}$ phase transits to the semimetallic state because one of the energy bands crosses the Fermi level on the segment between high-symmetry points Γ and V in the k-space, which

can be seen from the electronic band structure demonstrated in Fig. 5b.

As the pressure increases, the semimetallic state of the $P\bar{1}$ structure is maintained, and with a further increase in the pressure to 100 GPa, it is characterized by the presence of the band structure features similar to Dirac cones. These features are observed at high symmetry points X and Y in the k-space (see Fig. 6). For comparison, in the pressure range of 0−200 GPa,
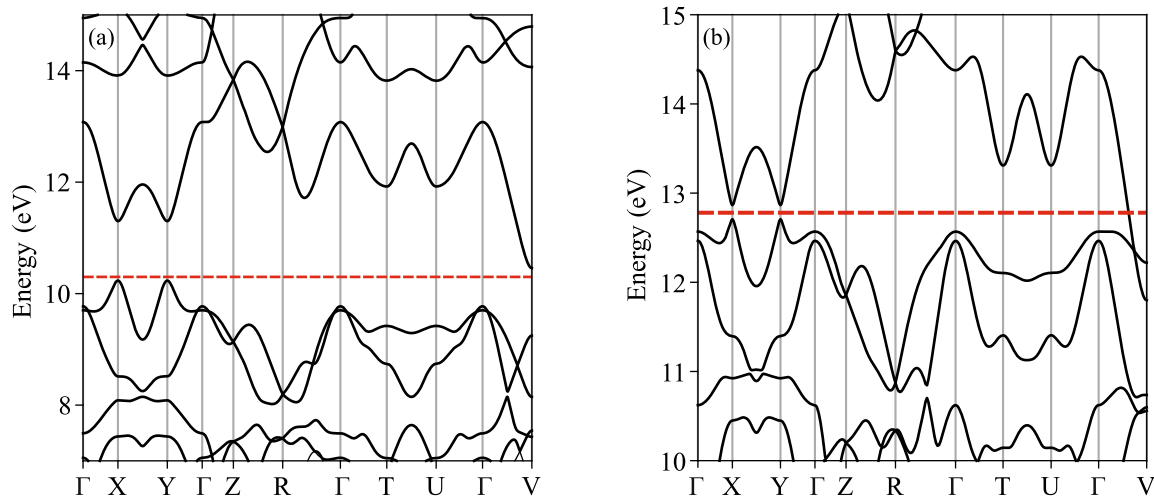

Fig. 5. (Color online) Electronic band structure for the solid atomic phase of nitrogen with the crystal lattice symmetry $P\bar{1}$ at pressures of (a) 20 and (b) 50 GPa. The position of the Fermi level is marked by the red dashed line.
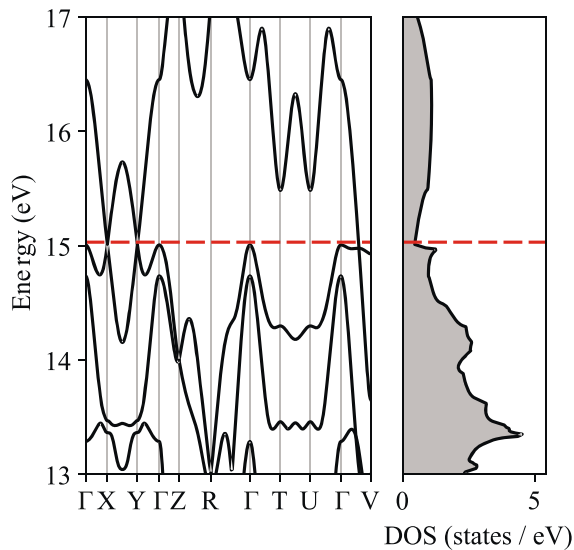
Fig. 6. (Color online) Electronic band structure and electron density of states for the $P\overline{1}$ phase at a pressure of 100 GPa. The position of the Fermi level is indicated by the red dashed line.

the cg-N phase is an insulator with a band gap of ≥ 4 eV, and the band gap in the nitrogen phases cg-N, $Pccn$, and $R\overline{3}$ increases with the pressure up to 100 GPa, and at higher pressures, the band gap begins to gradually decrease. However, because of the high rigidity of the bonds in nitrogen structures (these structures have large values of the bulk modulus ~200−280 GPa), their structural and electronic properties change slowly with increasing pressure. This makes it possible, e.g., in the case of the $R\overline{3}$ phase, to reach the metallic state only at ultrahigh pressures, exceeding 400 GPa.

Table 2. Bulk modulus of elasticity B, Young's modulus E, shear modulus G, and Poisson ratio n of solid atomic phases $P\overline{1}$ and cg-N of nitrogen at indicated pressures P

Elastic moduli	$P =$ 20 GPa	$P =$ 50 GPa	$P =$ 100 GPa	$P =$ 200 GPa
$B_{P\overline{1}}$, GPa	231	372	558	896
$E_{P\overline{1}}$, GPa	405	552	702	908
$G_{P\overline{1}}$, GPa	167	220	272	342
$n_{P\overline{1}}$, GPa	0.21	0.25	0.29	0.33
$B_{cg\text{-}N}$, GPa	284	451	610	910
$E_{cg\text{-}N}$, GPa	585	780	920	1086
$G_{cg\text{-}N}$, GPa	253	322	368	418
$n_{cg\text{-}N}$, GPa	0.16	0.21	0.25	0.30

CONCLUSIONS

A new solid phase of nitrogen, which is dynamically stable at pressures above 20 GPa, has been discovered by modeling the process of adiabatic compression at zero temperature for a crystal structure formed by two $N_6(C_{2v})$-A clusters. This structure has the crystal lattice symmetry $P\overline{1}$ and exhibits electronic properties unique for such systems, which characterize it as a semimetal at sufficiently low pressures, starting from 50 GPa and higher. At pressures of ~100 GPa, a semimetallic state is formed by two features on the electronic band structure characteristic of Dirac cones. The study of these features requires separate consideration. Owing to the rigidity of covalent bonds, this semimetallic state is maintained even when the pressure is increased to 200 GPa. This phase should be opaque to optical radiation of the corresponding wavelength, in contrast to the gauche phase of nitrogen. The results of the work also show that nitrogen clusters are of interest not only as independent objects of research but also as precursors for obtaining solid atomic phases of nitrogen.

FUNDING

CONFLICT OF INTEREST

The authors declare that they have no conflicts of interest.

OPEN ACCESS

REFERENCES

1. V. E. Zarko, Combust. Explos. Shock Waves **46**, 121 (2010).

2. H. H. Krause, New Energetic Materials, in *Energetic Materials: Particle Processing and Characterization* (Wiley-VCH, Weinheim, 2005), Chap. 1, p. 1.

3. F. Cacace, G. de Petris, and A. Troiani, Science (Washington, DC, U. S.) **295**, 480 (2002).

4. A. Vij, J. G. Pavlovich, W. W. Wilson, V. Vij, and K. O. Christe, Angew. Chem. Int. Ed. **41**, 3051 (2002).

5. K. O. Christe, W. W. Wilson, J. A. Sheehy, and J. A. Boatz, Angew. Chem. Int. Ed. **38**, 2004 (1999).

6. S. Fau, K. J. Wilson, and R. J. Bartlett, J. Phys. Chem. A **106**, 4639 (2002).

7. L. J. Wang, P. G. Mezey, and M. Z. Zgierski, Chem. Phys. Lett. **391**, 338 (2004).

8. D. L. Strout, J. Phys. Chem. A **108**, 2555 (2004).

9. H. Zhou, N.-B. Wong, G. Zhou, and A. Tian, J. Phys. Chem. A **110**, 3845 (2006).

10. M. R. Manaa, Chem. Phys. Lett. **331**, 262 (2000).

11. H. Zhou, N.-B. Wong, G. Zhou, and A. Tian, J. Phys. Chem. A **110**, 7441 (2006).

12. H. Zhou, N.-B. Wong, and A. Tian, J. Mol. Graphics Model. **25**, 578 (2006).

13. A. C. R. Gomes, M. X. Silva, and B. R. L. Galvão, RSC Adv. **11**, 21567 (2021).

14. S. Duwal, Y.-J. Ryu, M. Kim, C.-S. Yoo, S. Bang, K. Kim, and N. H. Hur, J. Chem. Phys. **148**, 134310 (2018).

15. E. E. Rennie and P. M. Mayer, J. Chem. Phys. **120**, 10561 (2004).

16. T. M. Klapötke, in *High Energy Density Materials* (Springer, Berlin, 2007), p. 85.

17. C. Mailhiot, L. H. Yang, and A. K. McMahan, Phys. Rev. B **46**, 14419 (1992).

18. M. M. G. Alemany and J. L. Martins, Phys. Rev. B **68**, 024110 (2003).

19. W. D. Mattson, D. Sanchez-Portal, S. Chiesa, and R. M. Martin, Phys. Rev. Lett. **93**, 125501 (2004).

20. F. Zahariev, A. Hu, J. Hooper, F. Zhang, and T. Woo, Phys. Rev. B **72**, 214108 (2005).

21. A. R. Oganov and C. W. Glass, J. Chem. Phys. **124**, 244704 (2006).

22. J. Sun, M. Martinez-Canales, D. D. Klug, C. J. Pickard, and R. J. Needs, Phys. Rev. Lett. **111**, 175502 (2013).

23. A. A. Adeleke, M. J. Greschner, A. Majumdar, B. Wan, H. Liu, Z. Li, H. Gou, and Y. Yao, Phys. Rev. B **96**, 224104 (2017).

24. S. V. Bondarchuk and B. F. Minaev, Phys. Chem. Chem. Phys. **19**, 6698 (2017).

25. K. S. Grishakov and N. N. Degtyarenko, JETP Lett. **112**, 630 (2020).

26. K. Grishakov, K. Katin, M. Gimaldinova, and M. Maslov, Lett. Mater. **9**, 366 (2019).

27. F. Zahariev, J. Hooper, S. Alavi, F. Zhang, and T. K. Woo, Phys. Rev. B **75**, 140101(R) (2007).

28. Y. Ma, A. R. Oganov, Z. Li, Y. Xie, and J. Kotakoski, Phys. Rev. Lett. **102**, 065501 (2009).

29. M. I. Eremets, R. J. Hemley, H. Mao, and E. Gregoryanz, Nature (London, U.K.) **411**, 170 (2001).

30. M. I. Eremets, A. G. Gavriliuk, N. R. Serebryanaya, I. A. Trojan, D. A. Dzivenko, R. Boehler, H. K. Mao, and R. J. Hemley, J. Chem. Phys. **121**, 11296 (2004).

31. M. I. Eremets, A. G. Gavriliuk, I. A. Trojan, D. A. Dzivenko, and R. Boehler, Nat. Mater. **3**, 558 (2004).

32. D. Tomasino, M. Kim, J. Smith, and C.-S. Yoo, Phys. Rev. Lett. **113**, 205502 (2014).

33. D. Laniel, B. Winkler, T. Fedotenko, A. Pakhomova, S. Chariton, V. Milman, V. Prakapenka, L. Dubrovinsky, and N. Dubrovinskaia, Phys. Rev. Lett. **124**, 216001 (2020).

34. D. Laniel, G. Geneste, G. Weck, M. Mezouar, and P. Loubeyre, Phys. Rev. Lett. **122**, 066001 (2019).

35. P. Giannozzi, S. Baroni, N. Bonini, et al., J. Phys.: Condens. Matter **21**, 395502 (2009).

36. P. Giannozzi, O. Andreussi, T. Brumme, et al., J. Phys.: Condens. Matter **29**, 465901 (2017).

37. D. R. Hamann, Phys. Rev. B **88**, 085117 (2013).

38. https://dalcorso.github.io/thermo_pw for informationabout the thermo_pw software.

39. Y. Hinuma, G. Pizzi, Y. Kumagai, F. Oba, and I. Tanaka, Comput. Mater. Sci. **128**, 140 (2017).

Translated by R. Bando